Available online at www.sciencedirect.com

ScienceDirect

Acta Materialia 82 (2015) 155–166

Acta MATERIALIA

www.elsevier.com/locate/actamat

Kinetics and anisotropy of the Monte Carlo model of grain growth

J.K. Mason,[a,b] J. Lind,[a,*] S.F. Li,[a] B.W. Reed[a] and M. Kumar[a]

[a]*Lawrence Livermore National Laboratory, Livermore, CA 94550, USA*
[b]*Boğaziçi University, Bebek, Istanbul 34342, Turkey*

Received 14 May 2014; revised 2 August 2014; accepted 25 August 2014
Available online 4 October 2014

Abstract—The Monte Carlo model is one of the most frequently used approaches to simulate grain growth, and retains a number of features that derive from the closely related Ising and Potts models. The suitability of these features for the simulation of grain growth is examined, and several modifications to the Hamiltonian and transition probability function are proposed. The resulting model is shown to not only reproduce the usual behaviors of grain growth simulations, but to substantially reduce the effect of the underlying pixel lattice on the microstructure as compared to contemporary simulations.

Keywords: Grain growth; Monte Carlo method; MC simulations; Computer simulation

1. Introduction

The Monte Carlo (MC) method is one of the main computational approaches used in the study of grain growth and related phenomena, and has provided useful qualitative insights into these processes for several decades. Derived from the Ising and Potts models of ferromagnetic systems, MC models represent a material as a collection of area or volume elements endowed with spins and arranged on a regular lattice. A grain is defined as a contiguous collection of material elements with the same spin, and the microstructure is evolved by probabilistic rules to propagate the spin of a given element to the neighboring ones.

Originally formulated in the context of microstructure evolution by Anderson et al. [1], the MC model quickly proved useful in the study of the grain growth microstructure [2], of stagnation in the presence of second-phase particles [3], of the effect of anisotropic boundary energies [4], and of the factors leading to abnormal grain growth [5–7]. Furthermore, the relative simplicity of the formulation allowed various implementations of the model to be extended for other purposes as well. For example, three-dimensional versions have been used to investigate the variations in grain structure around welds [8] and the effect of texture and texture evolution during grain growth on the microstructure [9], to evaluate a mean-field theory for the grain size distribution [10], and to support an analytical model for disordered cellular structures inspired by thermodynamic considerations [11].

Certain modifications of the underlying algorithm have been proposed to improve the computational efficiency of the model. The most important of these is the kinetic MC method, occasionally known in the materials science literature as the *n*-fold way algorithm. The fundamental observation is that using a variable time step equal to the interval required for the system configuration to change is often more efficient than using a constant time step and repeatedly proposing changes that may be rejected. While initially developed for the Ising model [12], the same approach may be applied to the MC model of grain growth [13]. This has the additional advantage that the kinetic MC method is readily parallelized [14,15], allowing the simulation of statistically significant volumes of material.

Unfortunately, the standard formulation of the MC model should not be used if predictive simulations of material behavior are required [16]. There are three main reasons for this assertion. First, the probabilistic rules used by the Monte Carlo method to update the system configuration do not have any physical basis. When initially formulated by Metropolis et al. [17], the purpose of the MC method was to model the distribution of states of a microscopic system in thermodynamic equilibrium. The rule for changing the configuration was chosen on the basis of mathematical simplicity, subject to the condition that the system sample states are at frequencies consistent with the canonical ensemble. By contrast, a microstructure is a macroscopic system far from thermodynamic equilibrium. A change of configuration is interpreted as grain boundary migration and should be subject to the corresponding

* Corresponding author; e-mail addresses: jeremy.mason@boun.edu.tr; lind9@llnl.gov; li31@llnl.gov; reed12@llnl.gov; kumar3@llnl.gov

http://dx.doi.org/10.1016/j.actamat.2014.08.063
1359-6462/

kinetics, not to relations defined only for mathematical convenience.

Second, the quantities appearing in MC models do not have well-defined units, precluding the direct comparison of simulation results with experiments. For example, material elements have arbitrary spatial dimensions, time is measured in arbitrary units, and the temperature appearing in the Metropolis dynamics is meaningful only in the context of the type of simulations performed by Metropolis et al. [17]. This situation is caused by the absence of any suitable kinetic relations in the formulation of the model. While at least one analytic [18] and several numerical [19,20] approaches to assign units to the simulations have been proposed, none appears to have been widely adopted by the computational materials science community.

Third, the use of a lattice of material elements introduces an inherent anisotropy into the simulations. This causes various unphysical phenomena, including grain boundary faceting, deviations of the dihedral angles along triple lines, and grain growth stagnation. The consensus in the literature [21–24] seems to be that the anisotropy may be mitigated by carefully selecting the underlying lattice, by using a fictitious temperature high enough to introduce limited grain boundary roughening, or by increasing the interaction cutoff distance between material elements. None of these is entirely satisfactory though. The number of available lattices is limited, the temperature must be calibrated to balance the effects of unphysical boundary faceting with unphysical boundary roughening, and increasing the interaction distance dramatically accelerates the disappearance of small microstructural features.

The primary purpose of this paper is to reduce the inherent anisotropy of the MC model. Since the absence of a physical basis for the standard MC model means that nothing is sacrosanct, we make two modifications to the underlying algorithm. First, the strength of the element interactions is allowed to vary as a function of the element separation, rather than being a constant for all elements within the cutoff distance. Second, the configuration is updated by choosing one of several proposed configurations with a function that depends smoothly on the energy change, rather than accepting or rejecting a single proposed configuration with a function constructed only for mathematical convenience.

The performance of the modified MC model is compared to that of a standard MC model by analyzing the microstructures resulting from grain growth simulations. Specifically, we consider the distribution of grain boundary normal directions and the deviations of the rate of change of grain areas from the von Neumann–Mullins relation [25,26]. Comparing these with corresponding quantities for a truly isotropic material reveals that the modified MC model reduces the inherent anisotropy of the lattice significantly more than the standard MC model, and is therefore preferable to the standard MC model in practice.

2. Traditional Monte Carlo

The history of the MC method is briefly reviewed, with particular emphasis on the source of the algorithm. This will help to identify a set of features that may safely be changed without violating any fundamental mathematical or thermodynamic constraints, and serves as motivation for the modifications to the algorithm proposed in Section 3.

2.1. Ising and Potts models

The Ising and Potts models are mathematical models most often used to study phase transitions in ferromagnetic systems, and have a long history in statistical physics [27]. Assume that a regular lattice of particles endowed with magnetic spins inhabits a two-dimensional (2-D) region with periodic boundary conditions. The spin of a given particle interacts magnetically with the spins of neighboring particles, and possibly with an external magnetic field.

The study of this system is usually restricted to the expected distribution of states in the canonical ensemble. The interaction of neighboring particles effectively precludes an analytical solution, however [28], meaning that the expected distribution of states is usually evaluated by sampling as a given configuration moves through the state space. A set of rules to guide the evolution of the initial configuration is provided by either Glauber dynamics [29] or Metropolis dynamics [17].

The Ising and Potts models (and MC grain growth models) are customarily described within the framework of the Metropolis algorithm. This means that the usual formulations have the following three features:

1. The Hamiltonian provides the energy of a configuration of the system. It is generally constructed from the sum of finite-range pairwise interactions and should be non-negative, bounded and translation invariant.
2. The proposal distribution is the conditional probability distribution of the proposed configuration of the system in the following time step, given the current system configuration. It is often assumed to be a uniform distribution on the adjacent states in the configuration space.
3. The acceptance distribution (often known as the transition probability) is the conditional probability to accept the proposed configuration of the system in the following time step, given the current system configuration.

These three features of the Ising and Potts models will be described in further detail below to help clarify the historical underpinnings of the MC grain growth model.

The Hamiltonian used by the Ising and Potts models in the absence of an external magnetic field is most often of the form:

$$H = \frac{1}{2}\sum_i J \sum_j (1 - \delta_{s_i s_j}), \tag{1}$$

where the outer sum is performed over all spins, J is the energy penalty between spins of different orientations, the inner sum is performed over the spins in a standard neighborhood around the ith spin, and $\delta_{s_i s_j}$ is the Kroneker delta, equal to one whenever the states s_i and s_j of the ith and jth spins are the same and to zero otherwise. Notice that the energy of a configuration with all spins aligned is zero, and that the energy penalty for spins of different states is halved in Eq. (1) because of double-counting.

The inner summation in Eq. (1) will be called the kernel of the Hamiltonian, while the coefficient of the kernel will be called the energetic coefficient and the argument of the inner summation will be called the weighting function. The kernel is distinguished by being closely related to the change in the energy of the system when the state of a single spin is changed. Specifically, changing the state of the ith spin changes the system energy by:

$$\Delta H = J\left[\sum_j (1-\delta_{s_i^1 s_j}) - \sum_j (1-\delta_{s_i^0 s_j})\right], \tag{2}$$

where s_i^0 is the initial state and s_i^1 is the final state. Notice that this is simply the difference in the appropriate kernels multiplied by the energetic coefficient.

The proposal and acceptance distributions are usually formulated to satisfy a technical condition known as detailed balance. Suppose, as in the Metropolis algorithm [17], that the model is interpreted as sampling the allowed microstates of a physical system that obeys the canonical ensemble. Then the probability of observing a particular microstate x_a is:

$$p_a \propto \exp\left(-\frac{H_a}{k_B T}\right), \tag{3}$$

where H_a is the Hamiltonian evaluated for state x_a, k_B is Boltzmann's constant, T is the absolute temperature, and the constant of proportionality is the partition function. This system satisfies detailed balance provided that the proposal distribution and acceptance distribution are such that the probability of being in state x_a and transitioning to state x_b is the same as the probability of being in state x_b and transitioning to state x_a.

Within the literature, the proposal distribution is usually a uniform distribution over the adjacent states in the configuration space. That is, a spin and a proposed state for that spin are randomly selected, subject to the condition that the proposed state be different from the current one, and the resulting energy change is calculated from Eq. (2). Given this proposal distribution, one of two acceptance distributions is often used. The Metropolis function [17]

$$w = \begin{cases} \exp\left(-\frac{\Delta H}{k_B T}\right) & \text{if } \Delta H > 0 \\ 1 & \text{if } \Delta H \leqslant 0 \end{cases} \tag{4}$$

is the simpler of the two, and has the advantage of historical precedence. By contrast, the Glauber function [29]

$$w = \frac{1}{1+\exp\left(\frac{\Delta H}{k_B T}\right)} \tag{5}$$

has more physical motivation, and has the advantage of being a smooth function of the energy difference. Both satisfy the conditions of ergodicity and detailed balance, though the Metropolis function appears more frequently in the literature.

2.2. Monte Carlo grain growth

While the Ising and Potts models do not correspond to any physical system, given a suitable initial condition the procedure described above does result in the growth of domains containing particles with aligned spins. Visually, these domains resemble grains in a 2-D material enough to suggest an alternative interpretation of the model.

Let the lattice of particles correspond to the pixels of a 2-D material, and let the state of a spin correspond to the crystal orientation of the pixel. With these modifications, the model described above may be used as a simple model of grain growth. However, the following points should be emphasized:

1. The dynamics of this system is strongly dependent on the choice of kernel. Small neighborhoods generally result in structures that do not resemble microstructures. While the kernel from Eq. (1) is often used, this has no particular physical motivation.
2. The Metropolis transition function is purely a convenient mathematical choice when attempting to measure the stationary distribution on a configuration space, and has no particular physical motivation.
3. Interpreting the model in the context of grain growth requires the configuration space to consist of macrostates instead of microstates, calling into question the initial assumption that the system obey the canonical ensemble.
4. Units of length and time do not appear anywhere in the model, and as a result the temperature in Eq. (4) is fictitious. Various attempts have been made to relate the simulations to experiments [18–20], though these have not been widely adopted.

While the first and second points have been noticed and commented upon by other authors, there does not appear to be any literature in the context of grain growth that acknowledges the third. This is particularly troublesome for the study of grain growth, in which the initial state of the system guarantees evolution in a certain direction (i.e. towards larger grain sizes) and is therefore necessarily far from thermodynamic equilibrium. There is little reason to assume that a simulation formalism designed to guarantee a correct statistical sampling of near-equilibrium states will also produce physically realistic dynamics in states far from equilibrium. The fourth requires a lengthy discussion that will be postponed for a future publication.

Provided that the subject of study is the qualitative behavior of a material, the above concerns should not prevent the use of the MC grain growth model. This is particularly the case when simulating the behavior of a simplified material, e.g. one with a constant grain boundary energy function, since this means that there is no experimental basis for comparison. As soon as the purpose is to simulate realistic material behavior though, the specifics of the energetics and kinetics should be carefully considered.

3. Revised Monte Carlo

This section suggests several changes to the traditional MC grain growth algorithm. Specifically, we propose changes to the kernel and transition function that break the historical connections to the Ising and Potts models, but appear to be more physically motivated in the context of grain growth. Our changes should nevertheless be relatively simple to incorporate into existing codes.

3.1. Smooth Kernel

MC grain growth simulations are generally performed on a lattice of elements. Since the process of grain growth in a material with a uniform boundary energy is isotropic and the underlying lattice is inherently anisotropic, various techniques have been developed to reduce the magnitude of the anisotropy. Foremost among these is increasing the number of pixels included in the kernel of the Hamiltonian, since making the interacting neighborhood more circular generally reduces the effect of the lattice on the energy

calculation. That is, the motivation for this change is to make the kernel as nearly a radial function as possible.

The fundamental purpose of the kernel is to transform the energetic contribution of surface elements along a grain boundary into a volumetric contribution from the pairwise interaction of pixels. This is necessary since a pixel is the elementary unit of the simulation, and a pixel corresponds to a discrete volume of material. Hence, we desire a kernel of the same form as in Eq. (1), but with the following properties:

1. The kernel should not identify any particular direction in space, i.e. the weighting function should be as close to a radial function as is possible on a lattice.
2. The weighting function should give more weight to nearby pixels since these are presumably more relevant to the local configuration.
3. The weighting function should smoothly decrease to zero at the edge of the kernel neighborhood to reduce the effect of the choice of cutoff distance on the dynamics.

This suggests that the weighting function be based on the discrete sampling of a continuous radial function, e.g. a Gaussian. For convenience of notation, the value of the Gaussian centered on $\vec{r}_i$, the coordinates of the ith pixel, and evaluated on $\vec{r}_j$, the coordinates of the jth pixel, will be written as:

$$F_{ij} = \exp\left(-\frac{|\vec{r}_j - \vec{r}_i|^2}{2\sigma^2}\right). \tag{6}$$

Notice that F_{ij} depends on the standard deviation σ, and that the standard deviation is expressed in the same units as the coordinates of a pixel. Let q_i be the unique label for the grain containing the ith pixel. With this, the kernel N_i around the ith pixel may be written as:

$$K_i = \frac{\sum_{j:F_{ij}\geqslant c} F_{ij}(1-\delta_{q_i q_j})}{\sum_{j:F_{ij}\geqslant c} F_{ij}}, \tag{7}$$

where the summations are performed over pixels with weights above the cutoff value c, and $\delta_{q_i q_j}$ is the Kroneker delta. The summation is normalized in an effort to make the magnitude of the energetic contribution of a pixel independent of σ and c. Based on the same reasoning as in Eq. (2), the energy change of the system resulting from changing the orientation of the ith pixel is given by the difference of the nuclei. That is,

$$\Delta H = \gamma(K_i^1 - K_i^0), \tag{8}$$

where γ is a constant energetic coefficient, K_i^0 is the kernel in the initial state, and K_i^1 is the kernel in the final state. The performance of the proposed kernel and appropriate values of σ and c will be considered in Section 4.

3.2. Weighted transitions

The traditional formulation of the MC grain growth algorithm stipulates that one pixel be selected uniformly at random from the lattice, and that one proposed state be selected uniformly at random from the entire set of permissible states. After calculating the energy difference between the current state and the proposed state, the proposed state is accepted on the basis of the Metropolis function. This has the advantages of simplicity and of satisfying detailed balance.

Early practitioners observed, however, that the majority of proposed states resulted in substantial energy increases, resulting in relatively few accepted changes. The reason for this phenomenon is that a pixel will more often change orientation to that of one of the neighboring grains (resulting in boundary motion) than change to a completely different orientation (resulting in grain nucleation). As a result, the simulation may often be accelerated with only minimal changes to the final state by selecting the proposed state uniformly at random from the set of neighboring orientations and excluding the initial orientation of the pixel. While this violates detailed balance, the relaxed relationship between the model and the statistical mechanical underpinnings means that this violation does not necessarily invalidate the results.

The dynamics described above sample all of the orientations adjacent to the pixel at the same frequency, regardless of the number of adjacent pixels with that orientation. Consider a pixel adjacent to a triple point for which the energy of the system is reduced by either one of the available reorientations, but more so by one than by the other. Using a uniform proposal distribution and a Metropolis acceptance distribution, the two available reorientations will be sampled with the same probability, and therefore will be accepted at the same probability since they both reduce the energy of the system. However, this contradicts a general principle for macroscopic systems that the driving force for an event is directly proportional to the accompanying energy reduction.

This suggests that the proposal and acceptance distributions be reformulated to apply the MC method to a macroscopic system. Specifically, select a pixel uniformly at random from the lattice, and assign the ith state from the entire set of permissible states to this pixel with probability

$$W_i = \frac{\exp\left(-\frac{\Delta H_i}{k_B T}\right)}{\sum_j \exp\left(-\frac{\Delta H_j}{k_B T}\right)}. \tag{9}$$

Notice that this effectively samples all of the permissible states simultaneously, but assigns weights to each according to the accompanying energy change. Since the current orientation of the pixel is included in the set, a reorientation event may effectively be rejected. Furthermore, the probabilities have the advantage of being smooth functions of the energy changes, and may be shown to satisfy detailed balance. This is effectively a hybrid of the sequential MC algorithm and the kinetic MC algorithm in that the relative probability of events is appropriately considered, but without the need to construct and maintain a table of all possible transition rates.

This scheme does have the disadvantage that considerable computational time is spent examining relatively improbable grain nucleation events. As with traditional MC, the simulation may be substantially accelerated by considering only the full set of neighboring orientations (including the initial orientation of the pixel) instead of the entire set of permissible states. Although the resulting dynamics violate detailed balance in precisely the same way as the standard MC model, we find that this change minimally affects the final state of the system.

3.3. Boundary normal calculation

The motivation to reduce the inherent anisotropy of the MC model comes from our desire to simulate grain

coarsening effects in real materials. This implies the use of a realistic grain boundary energy function [30] that includes the dependence of the energy on the boundary plane normal. This dependence is quite sharp for certain boundaries, meaning that the normal vector must be computed accurately to avoid unphysical phenomena during microstructure evolution. Although calculating a smoothly varying boundary normal in a system composed of discrete pixels is known to be difficult [31,32], the procedure described below is found to be robust to the lattice anisotropy and may be calculated at all points along the grain boundary in any dimension.

Roughly speaking, the boundary normal is found by constructing a cloud of weighted points along the boundary and performing principal component analysis on this point cloud. Concentrating on K_i, the kernel of the ith pixel, suppose that the jth pixel satisfies the condition $F_{ij} > c$ and that grains q_i and q_j share a boundary. We find all pairs of adjacent pixels within the region K_i such that one pixel is in grain q_i and the other is in grain q_j. A point is constructed from every pair of pixels by averaging the pixel coordinates, and is given a weight by averaging the values of the weighting function. A schematic of the resulting point cloud is given in Fig. 1.

Explicitly, the set S_{ij} of coordinates and weights for the point cloud on the boundary of grains q_i and q_j in the region of the ith pixel is given by:

$$S_{ij} = \left\{ \frac{\vec{r}_k + \vec{r}_l}{2}, \frac{F_{ik} + F_{il}}{2} \right\}, \tag{10}$$

where k and l range over all values such that $F_{ik} \geqslant c, F_{il} \geqslant c, q_k = q_i, q_l = q_j$, and the kth and lth pixels are adjacent. The normal direction is defined as the principal axis of the weighted point cloud with the smallest variance, and the weights serve to increase the importance of points near the ith pixel and smooth out the variation of the normal direction along the boundary.

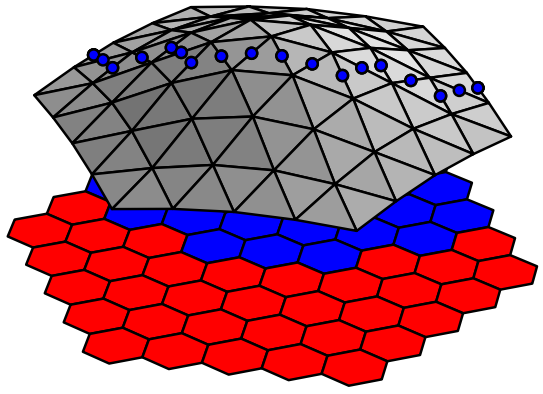

Fig. 1. A schematic representation of the point cloud on which principal component analysis is performed to calculate the grain boundary normal. Pixels within the interaction cutoff distance of the central pixel appear at the bottom of the figure, with the grain of the central pixel colored blue and the neighboring grain colored red. The grey surface is the weighting function of the smooth kernel. The blue points used in the principal component analysis are at the midpoints of the boundary segments between red and blue pixels, with weights interpolated from the weighting function. (For interpretation of the references to colour in this figure legend, the reader is referred to the web version of this article.)

4. Results and discussion

4.1. Simulation parameters

We have implemented the modifications proposed in Section 3, and have performed extensive 2-D MC grain growth simulations in a material with a uniform grain boundary energy to evaluate the performance of the modified MC model. This involved an exhaustive sweep through a parameter space that includes the temperature T, the standard deviation of the smooth kernel σ, and the interaction distance cutoff c. All simulations begin from the same initial condition, namely a microstructure composed of 9725 equiaxed grains on a hexagonal lattice containing $9,000,000$ pixels. To enable a comparison with the standard MC model, we perform a second set of simulations with a uniformly weighted kernel defined by:

$$K_i' = \frac{\sum_{j:\,|\vec{r}_j - \vec{r}_i| \leqslant c} (1 - \delta_{q_i q_j})}{\sum_{j:\,|\vec{r}_j - \vec{r}_i| \leqslant c} 1}, \tag{11}$$

where the strength of the interactions is constant for all pixels within the interaction cutoff distance c. Simulations with this kernel were performed for the same intervals of temperature T and for comparable kernel areas as for the modified MC model. Table 1 represents the scope of kernel type, sizes and temperatures investigated in this study. Since the MC model does not contain quantities with well-defined units, we simply set k_B and γ to 1.

Fig. 2 shows the evolution of the initial microstructure using the smooth kernel with $\sigma = 2\frac{1}{3}, c = 10^{-5}$ and $T = 10^{-8}$, resulting in around 100 final grains. The average grain size increased linearly with MC step number as demonstrated in Fig. 7, and all suitably scaled distributions remained invariant as expected in statistically self-similar growth; the distribution of grain radii divided by the average grain radius is roughly log-normal, while the distributions of topological quantities (e.g. the number of grains bounded by n triple points) remained fixed as demonstrated in Fig. 8. Deviations from the expected grain growth behaviors were, however, observed in simulations for certain combinations of kernel sizes and temperatures. One example is given in Fig. 3, where we consider the case of low temperature and small kernel size for both the smooth and uniform kernel. Whereas abnormal grain growth is observed for the smooth kernel in Fig. 3(a), the uniform kernel in Fig. 3(b) only resulted in slower grain growth while maintaining the grain size distribution. Generally normal grain growth, in a statistical sense, is observed in all but a few cases. For simulations performed with a small smooth kernel ($\sigma = 1$), this kind of abnormal growth was observed for lower temperatures ($T < 10^{-2}$). Increasing the temperature alleviated these effects as has been prescribed previously in the literature to overcome lattice anisotropy.

4.2. Boundary normal distribution

In physical systems where the interface energy is uniform, e.g. in a soap foam or materials with an isotropic grain boundary energy, the distribution of boundary normals is not expected to contain any preferred direction. However, the implementation of the MC method requires an underlying discretized lattice, which induces preferred directions irrespective of the physical model. This was

Table 1. Range of parameters studied in a series of Monte Carlo grain growth simulations.

Kernel type	Kernel size	Temperature
Uniform	$c = 1, 2, 3, 4, 5, 6, 7, 8, 9, 10$	$10^{-8}, 10^{-7}, 10^{-6}, 10^{-5}, 10^{-4}, 10^{-3}, 10^{-2}$
Smooth	$\sigma = 1, 1\frac{2}{3}, 2\frac{1}{3}, 3, 3\frac{2}{3}, 4\frac{1}{3}, 5$ $c = 10^{-5}, 10^{-4}, 10^{-3}, 10^{-2}$	$10^{-8}, 10^{-7}, 10^{-6}, 10^{-5}, 10^{-4}, 10^{-3}, 10^{-2}$

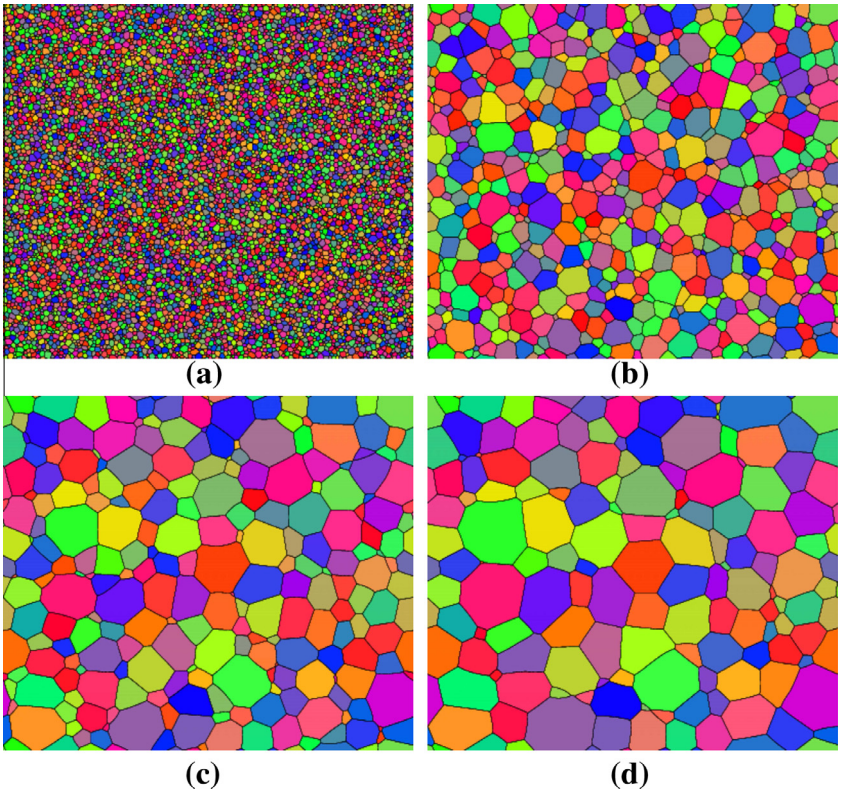

Fig. 2. Snapshots of a single grain growth simulation at (a) 0 MCS, (b) 600 MCS, (c) 1300 MCS and (d) 2000 MCS. A smooth kernel was used with parameters $\sigma = 2\frac{1}{3}, c = 10^{-5}$ and $T = 10^{-8}$.

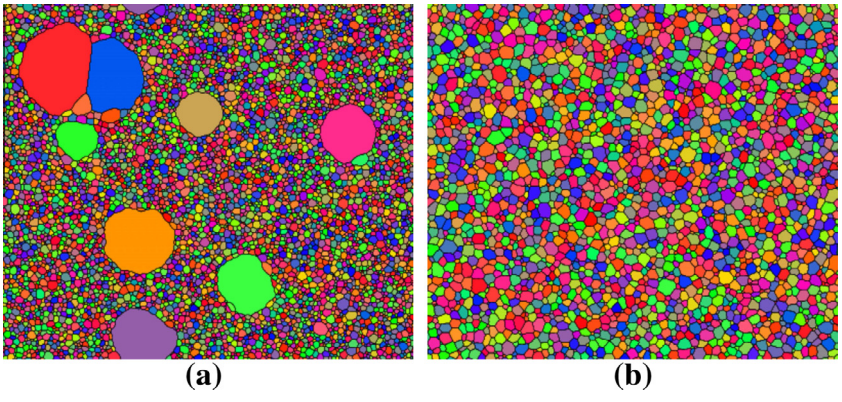

Fig. 3. Snapshots of two grain growth simulations started from the microstructure in Fig. 2(a) after 2000 MCS. (a) uses a smooth kernel with $\sigma = 1, c = 10^{-5}$ and $T = 10^{-8}$. (b) uses a uniform kernel with a cutoff of $R = 1$ lattice unit and $T = 10^{-8}$.

observed in a dramatic fashion by Anderson et al. [1]; in this case, the boundaries of grains conformed almost exactly to the simulated square grid. In general, the efficacy of a MC grain growth simulation depends heavily on the ability to quantify and minimize the effects of lattice anisotropy on the simulated microstructure.

Isotropic grain growth implies that a uniform boundary normal distribution (BND) should develop for a statistically representative sample, i.e. one where the number of grains is sufficiently large to make the counting error negligible. Hence, variations in the BND $n_{mc}(\theta)$, where θ is the angle of the normal with respect to the x-axis modulo

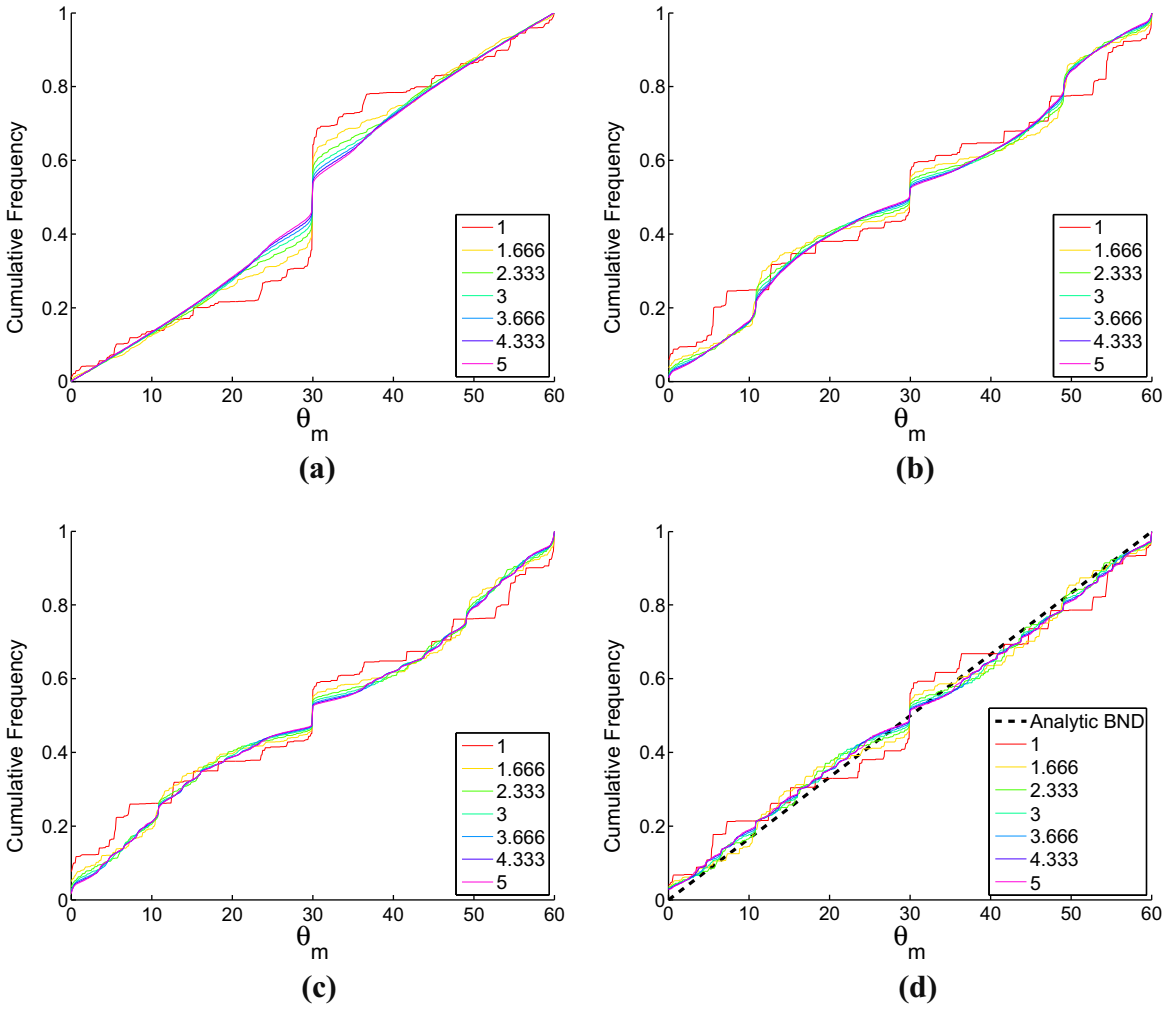

Fig. 4. Cumulative plots of the boundary normal distribution in a MC evolved microstructure when only 3000 grains remain using (a) a uniform kernel with $R = 1$ lattice unit and $T = 10^{-8}$, (b) a uniform kernel with $R = 3$ lattice units and $T = 10^{-8}$, and (c) a smooth kernel with $\sigma = 1\frac{2}{3}$, $c = 10^{-5}$ and $T = 10^{-8}$. (d) is the cumulative distribution of an ideally isotropic structure. The black dashed line corresponds to the uniform distribution. The legend indicates the size of the smooth kernel used to evaluate the boundary normals.

60°, allow the anisotropy of identical grain growth simulations with differing parameters to be quantified. More specifically, a single initial microstructure with 9725 grains was evolved using different sets of simulation parameters, and BNDs were all measured at the point where each of the simulations contained 3000 grains and had similar grain size distributions. The reduction in the number of grains by a factor of three ensures that the effects of the anisotropy are sufficiently reflected by the system configuration.

Unfortunately, the BND is also subject to the complicating effects of the measurement procedure itself. For example, the boundary normal at every point along a straight-line boundary in 2-D is by definition a constant. On the other hand, the boundary normal distribution for the same boundary in a discretized lattice has a non-negligible width, indicating deviations from the expected boundary normal distribution. That is, both the anisotropy introduced by the underlying lattice and the anisotropy introduced by normal estimation algorithm must be quantified.

The cumulative boundary normal distributions $N_{mc}(\theta)$ for selected simulations are shown in Fig. 4. Fig. 4(a) shows the case of a uniform kernel with $R = 1$, Fig. 4(b) shows the case of a uniform kernel with $R = 3$, and Fig. 4(c) shows the case of a smooth kernel with $\sigma = 1\frac{2}{3}$ and $c = 10^{-5}$. The temperature was 10^{-8} for all of these simulations. The different lines correspond to different σ of the smooth kernel used to estimate the boundary normals, as described in Section 3.3. Notice that a severe kink developed at 30° in all three cases, indicating an elevated probability of boundaries aligned with the hexagonal MC lattice. Increasing the size of the smooth kernel used in the boundary normal estimation procedure consistently reduces the strength of this discontinuity. Using the smooth kernel for the MC evolution, as in Fig. 4(c), results in a marked improvement as well, producing a generally more uniform distribution of boundary normals. By comparison, the uniform kernel produces secondary kinks at 11° and 49° as the size of the kernel is increased from Fig. 4(a) to (b). This implies that the uniform kernel does not monotonically converge to the ideally isotropic case with increasing kernel size, despite this being the usual procedure to reduce lattice anisotropy.

Fig. 4(d) shows the same boundary normal distribution for an ideally isotropic structure superimposed on a hexagonal lattice, and therefore indicates the systematic error introduced by the boundary normal estimation method. This is accomplished by first constructing a uniform

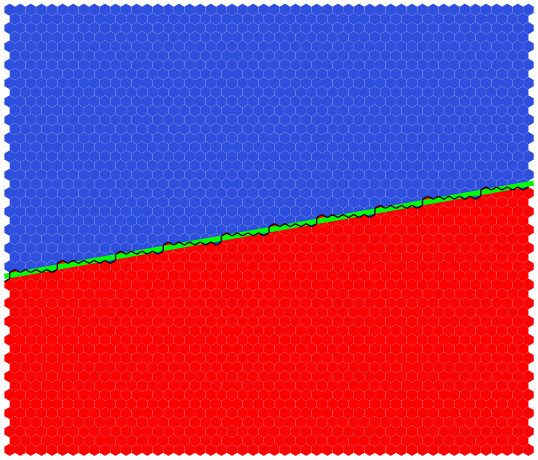

Fig. 5. A simulated boundary inclined 10° from the horizontal. The green line represents the continuous boundary. Note the stair-step behavior of the line mapped onto the discrete lattice by the black line which represents the interface between the blue and red regions. (For interpretation of the references to colour in this figure legend, the reader is referred to the web version of this article.)

sampling of boundaries with tilts ranging from 0° to 360° in steps of 0.1°. The boundaries are discretized on a hexagonal 2-D lattice that is large enough (200 × 200) to contain an appreciable number of facets. Fig. 5 shows an example of this process. Normal estimates are produced using the prescribed algorithm with smooth kernels of various sizes. As the size of the smooth kernel used to compute the normals is increased, the normal directions along the straight boundary converge to nearly a constant, i.e. the distribution of these normals becomes unimodal, continuous and minimally spread. Without analyzing the resulting distributions in detail, Fig. 4(d) shows a trend of the discretization effects being smoothed out as the size of the smooth kernel used for the normal estimation is increased. Given that the boundary tilts are uniformly sampled, the cumulative distribution for the boundary normal distribution would ideally be the straight line shown in black in Fig. 4(d). A simple comparison with the cumulative computed reference distributions suggests that the contribution of the boundary normal estimation to the apparent anisotropy is nontrivial. Overall, though, the method of normal calculation proposed in Section 3.3 appears to perform accurately and precisely when supplied with around 20 points along the boundary. This is in agreement with other methods used to estimate boundary inclination [32].

To separate this from the anisotropy due to the kernel used in the MC simulation, we calculate the sum-of-square difference between the reference cumulative distribution in Fig. 4(d) and the other cumulative distributions in Fig. 4. Explicitly, this sum of square difference is given by:

$$SSD = \sum_{\theta_i} [N_{rc}(\theta_i) - N_{mc}(\theta_i)]^2, \tag{12}$$

where θ_i is in the set of angles used in the binning procedure, and the results are presented in Table 2. For both the uniform kernel and the smooth kernel, the discrepancy reaches a comparatively small value in the range of 0.1–0.2 for the largest evolution kernels and normal estimation kernels, though for much larger values of R for the uniform kernel than of σ for the smooth kernel. Note that the SSD quantities in Table 2 are consistent with a qualitative comparison of the curves in Fig. 4. From this, we may conclude that both the underlying lattice type and the interaction kernel must be chosen carefully if the intention is to produce physically meaningful microstructures.

4.3. von Neumann–Mullins scaling

The von Neumann–Mullins relation (vNMR) relates the rate of area change of a grain to the number of triple points on the grain perimeter. The relation is exact in two dimensions for purely curvature-driven grain growth with an isotropic grain boundary energy function (i.e. all boundaries have the same energy per unit length). Specifically, the rate of area change for a grain with N triple points is:

$$\frac{dA_N}{dt} = K(N - N_0), \tag{13}$$

Table 2. Sum-of-squares difference (SSD) values between the measured cumulative boundary normal distributions, $N_{mc}(\theta)$, and the reference cumulative distributions, $N_{cr}(\theta)$, for various kernel types and sizes. Each row represents a specific kernel type used for the evolution of the Monte Carlo grain growth, and each column represents the size of the smooth kernel used for the estimation of normals.

Simulation type	Kernel size	PCA, $\sigma = 1$	$\sigma = 1\frac{2}{3}$	$\sigma = 2\frac{1}{3}$	$\sigma = 3$	$\sigma = 3\frac{2}{3}$	$\sigma = 4\frac{1}{3}$	$\sigma = 5$
Uniform	R = 1	4.755	3.671	2.778	2.372	2.146	2.030	1.963
Uniform	R = 2	1.541	1.342	0.908	0.611	0.451	0.345	0.279
Uniform	R = 3	0.513	0.485	0.547	0.495	0.456	0.420	0.399
Uniform	R = 4	0.245	0.232	0.397	0.458	0.484	0.494	0.501
Uniform	R = 5	0.164	0.167	0.240	0.332	0.388	0.419	0.441
Uniform	R = 6	0.113	0.182	0.287	0.396	0.484	0.542	0.586
Uniform	R = 7	0.173	0.095	0.090	0.092	0.106	0.121	0.132
Uniform	R = 8	0.160	0.121	0.118	0.126	0.141	0.154	0.170
Uniform	R = 9	0.122	0.103	0.095	0.109	0.127	0.142	0.161
Uniform	R = 10	0.091	0.096	0.101	0.127	0.149	0.172	0.195
Smooth	$\sigma = 1\frac{2}{3}$	0.800	0.610	0.585	0.521	0.479	0.445	0.421
Smooth	$\sigma = 2\frac{1}{3}$	0.290	0.169	0.175	0.180	0.190	0.193	0.200
Smooth	$\sigma = 3$	0.210	0.135	0.136	0.152	0.173	0.182	0.193
Smooth	$\sigma = 3\frac{2}{3}$	0.118	0.077	0.088	0.112	0.136	0.154	0.172
Smooth	$\sigma = 4\frac{1}{3}$	0.116	0.085	0.090	0.110	0.133	0.152	0.171
Smooth	$\sigma = 5$	0.125	0.122	0.117	0.137	0.160	0.180	0.202

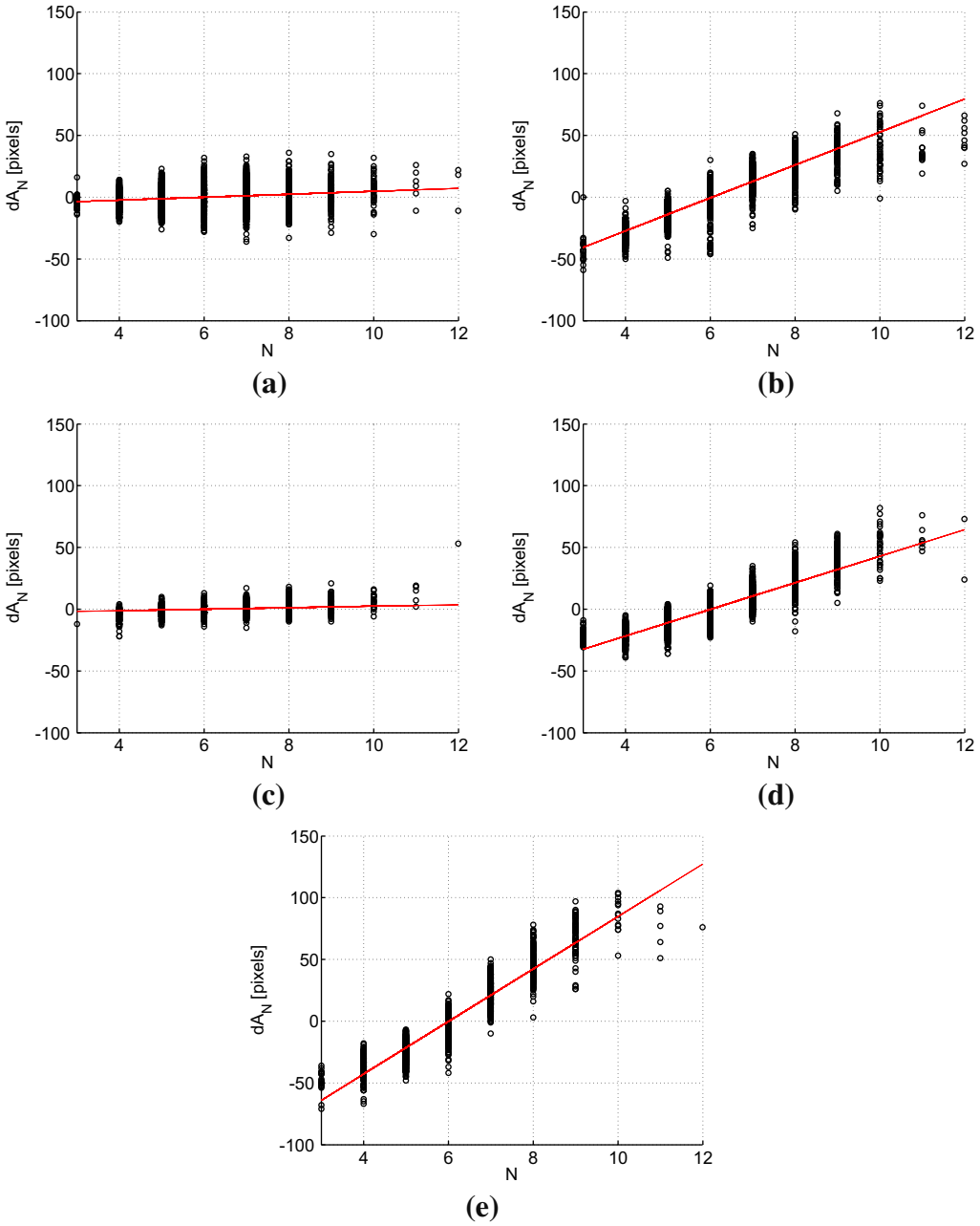

Fig. 6. von Neumann–Mullins relation plots showing the area changes for grains that do not experience a topological change in the entire simulated system between MCS = 99 and MCS = 100 for (a) a uniform kernel with $R = 1$ lattice unit, (b) a uniform kernel with $R = 5$ lattice units, (c) a small smooth kernel with $\sigma = 1$ and $c = 10^{-5}$, (d) a smooth kernel with $\sigma = 1\frac{2}{3}$ and $c = 10^{-5}$, and (e) a smooth kernel $\sigma = 3$ and $c = 10^{-5}$. Plots are shown on axes with consistent scale for comparison purposes. The red line represents the best fit to Eq. (13). (For interpretation of the references to colour in this figure legend, the reader is referred to the web version of this article.)

where K is the reduced mobility and N_0 is equal to 6, the number of triple points required for a grain's area to be constant. Combined with the assumption of self-similar growth, this implies that the area of an average grain should increase linearly in time ($<A> \propto t$), leading to a corresponding decay in the number of grains ($N_g \propto t^{-1}$). Although a sufficiently accurate simulation will satisfy the vNMR exactly for every grain on every time step, the usual practice for MC simulations is only to verify that it is satisfied on average for all grains with a given number of bounding triple points.

To evaluate the performance of our MC simulations, we track the number of triple points, the area change, and the total area of every grain on every MCS. The average reduced mobility K and the intercept N_0 are determined by a linear least-square fit using all grains with N bounding triple points where $4 \leqslant N \leqslant 12$. Fig. 6 shows how the simulation follows the von Neumann–Mullins law for a given simulation time. Fig. 7 shows the average grain size $<A>$ vs. MCS. For all simulated ranges of temperature, the simulations using the uniform kernel produce normal grain growth. That is, the intercept N_0 is consistently in the expected range about 6, the average reduced mobility K remains relatively constant, and the average grain size increases linearly in time and is thus consistent with curvature-driven grain growth.

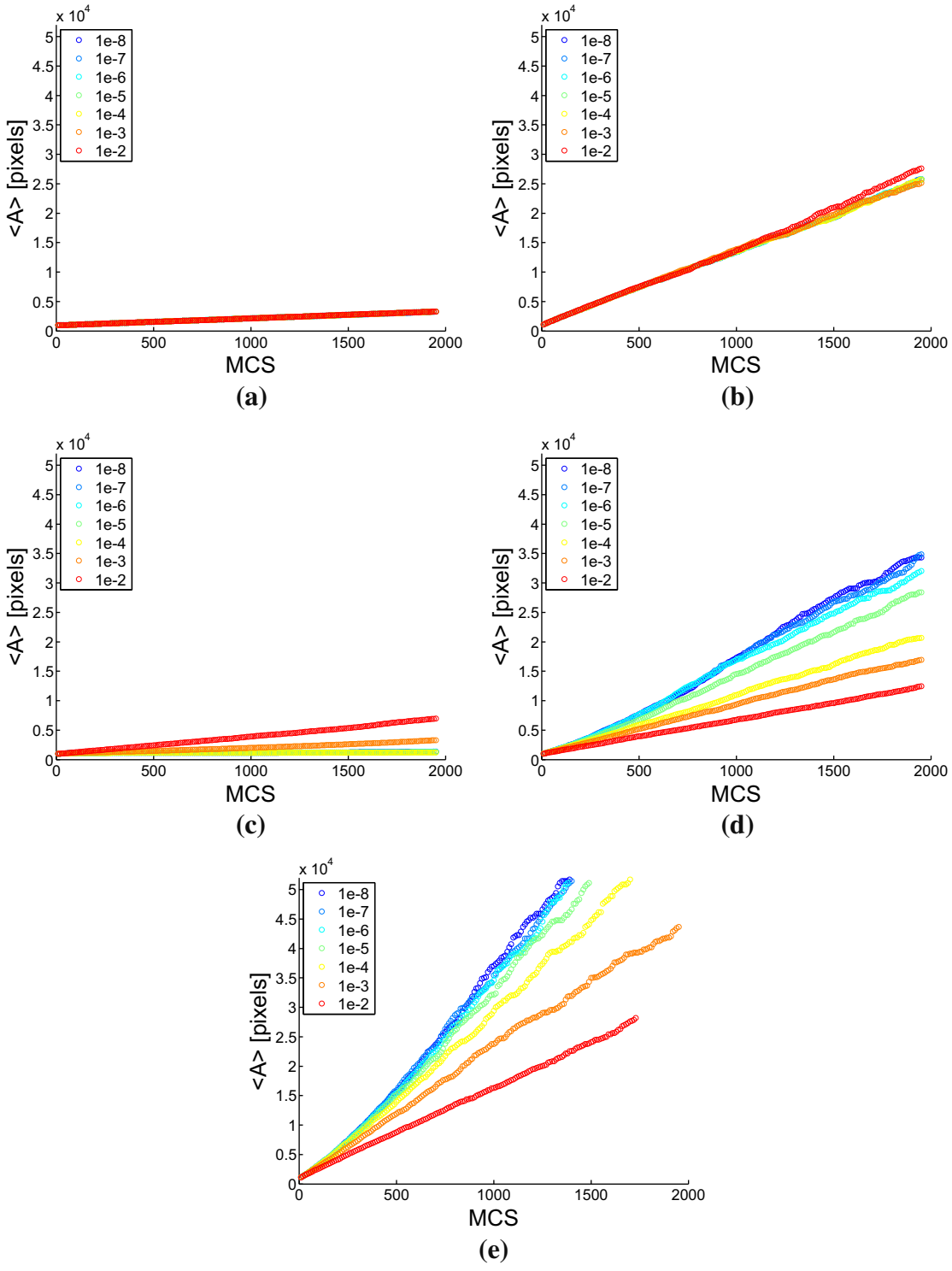

Fig. 7. Average grain size, $<A>$, for the entire simulated temperature range across 2000 MCS for (a) a uniform kernel with $R = 1$ lattice unit, (b) a uniform kernel with $R = 5$ lattice units, (c) a small smooth kernel with $\sigma = 1$ and $c = 10^{-5}$, (d) a smooth kernel with $\sigma = 1\frac{2}{3}$ and $c = 10^{-5}$, and (e) a smooth kernel $\sigma = 3$ and $c = 10^{-5}$. Plots are shown on axes with consistent scale for comparison purposes. The legend indicates the simulation temperature.

Two things are notable about Figs. 7(a) and (b), where the average area of a grain is plotted as a function of MCS for uniform kernels with $R = 1$ and $R = 5$, respectively. First, the rate of change of the average area increases strongly with increasing kernel size. This makes intuitive sense, since small grains tend to collapse when their radius is comparable to that of the kernel. Second, the average grain area in MC simulations using the uniform kernel shows almost no sensitivity to the temperature within the investigated interval. Given the temperature can be linked directly to the simulation lattice

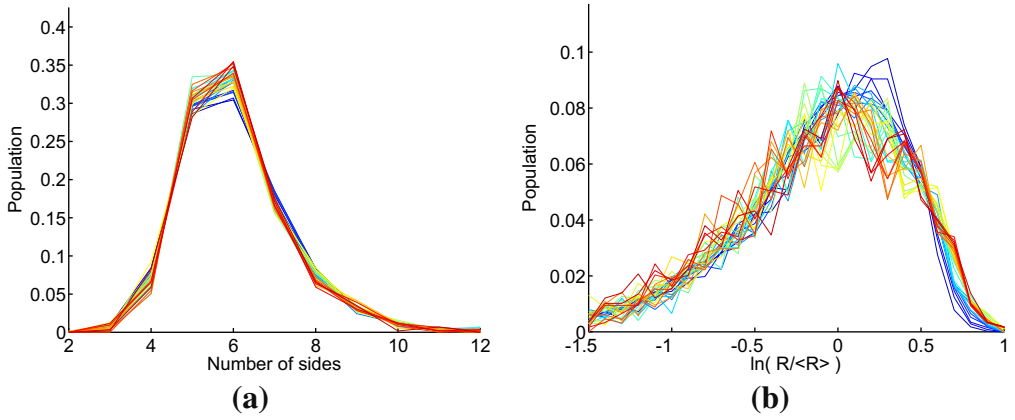

Fig. 8. Grain neighbor and size distribution for an example set of simulation parameters, $\sigma = 1\frac{2}{3}$, $c = 10^{-5}$, and $T = 10^{-4}$, where the number of grains in the system is reduced by a factor of 20. The coloring represents the distributions from early simulation time (blue) to later times (red). (For interpretation of the references to colour in this figure caption, the reader is referred to the web version of this article.)

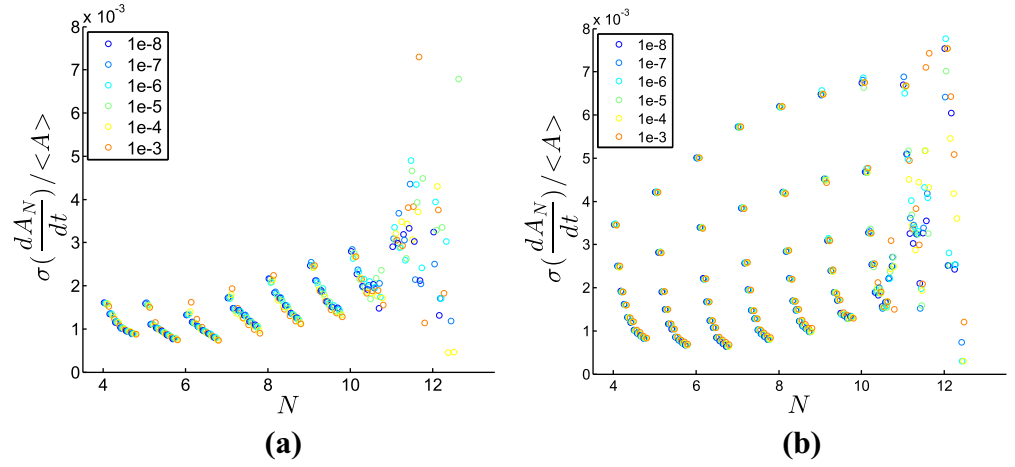

Fig. 9. Standard deviation in the rate of area change for grains with a given number of bounding triple points. (a) shows the results for a smooth kernel for $\sigma = 1\frac{2}{3}, 2\frac{1}{3}, 3, 3\frac{2}{3}, 4\frac{1}{3}$ and 5. (b) shows the results for a uniform kernel with $R = 1$ lattice unit to $R = 10$ lattice units. Between values of N, a marker indicates the standard deviation in $\frac{dA_N}{dt}$ normalized by the average grain size $<A>$, with increasing σ or R from left to right. The legend indicates the simulation temperature.

and kernel [24], the temperature range studied for the uniform kernel does not overcome the underlying lattice as evidenced by its insensitivity to temperature. At a reasonably higher temperature in which the lattice anisotropy is overcome, the trends for Figs. 7(a) and (b) would show similar temperature dependence to that of Figs. 7(d) and (e).

The behavior of the smooth kernel in Fig. 7 is quite different. For $\sigma = 1$ and $c = 10^{-5}$ in Fig. 7(c), the behavior changes drastically for temperatures between 10^{-4} and 10^{-3}, going from the abnormal grain growth visible in Fig. 3(a) to normal grain growth where K is nonzero, N_0 is around the ideal value of 6, and the average grain area increases linearly in time. For the smooth kernel with $\sigma = 1\frac{2}{3}$ and $c = 10^{-5}$ in Fig. 7(d), the average grain area increases linearly for a wide range of temperatures, and there is a noticeable trend of decreasing K with increasing T from 10^{-8} to 10^{-2}. This trend becomes even more evident as the smooth kernel is increased in size to $\sigma = 3$ with $c = 10^{-5}$ in Fig. 7(e). This may again be explained by the dependence of the average growth rate on the effective kernel size; as the temperature is lowered, the distance at which the pixel interaction strength is comparable to the fictitious thermal energy is shifted further out, increasing the effective radius of the kernel and the growth rate of the average grain.

While most sets of parameters satisfy the requirement that the average grain area increase linearly in time, the degree to which individual grains satisfy the vNMR depends more explicitly on the kernel size. Generally, given a collection of grains with N bounding triple points, the spread in rate of area change decreases with increasing kernel size. This implies that the simulation becomes more accurate as more information is used to determine boundary movement. Fig. 9 specifically shows that the standard deviation in the rate of area change for grains with a particular number of bounding triple points decreases with kernel size. The values of the rate of area change are scaled at each timestep by the average area to allow the values to be compared more directly. The plot shows the standard deviation over the entire simulation. Notice that the dependence of the deviation on the temperature, indicated by the color of the marker, is much smaller than the dependence on

the size of the kernel. This calls into question the frequent practice of increasing the temperature to improve the accuracy of the simulation.

5. Conclusion

The MC approach to grain growth simulations has already been in use for several decades, and has several notable advantages including a relative simplicity in implementation. However, caution must be exercised when attempting to extract physically relevant results from this type of simulation. The clearest reasons for this are the absence of dimensional quantities in the simulations and the inherent anisotropy of the underlying lattice, though there are some theoretical concerns as well. Our main concern here is to evaluate the magnitude of the inherent anisotropy, and to propose an alternative smooth kernel that helps to more rapidly reduce the anisotropy with increasing kernel size. Specifically, we find that.

- The traditional uniform kernel with nearest-neighbor interactions produces boundary inclination populations that are strongly influenced by the underlying simulation lattice. This effect is noticeably mitigated only when using uniform kernels of sizes much larger than those appearing in the literature.
- As indicated by Table 2, the proposed smooth kernel produces boundary normal populations comparable to those of the uniform one when the standard deviation σ of the smooth kernel is about half the value of the radius R of the uniform one.
- Both the uniform and the smooth kernels reproduce the expected linear dependence of the average grain area on time for suitable parameter values.
- As indicated by Fig. 9, the standard deviation of the growth rates of individual grains from the vNMR when using the proposed smooth kernel is comparable to that for the uniform one when the standard deviation σ of the smooth kernel is about half the value of the radius R of the uniform one.

If the purpose of a MC grain growth simulation is to explore the qualitative effect of some microstructural mechanism, then the effect of the inherent lattice anisotropy may well be small enough to be neglected. On the other hand, if the intention is to predict material behavior or to compare simulation directly with experiment, the lattice anisotropy must be carefully characterized and controlled. Our results indicate that, while the effect of the underlying lattice is considerable for a uniform kernel that includes only the neighboring pixels, the effect is gradually reduced as the size of the kernel is increased. Furthermore, the proposed smooth kernel with a given value of σ performs roughly as well as the uniform kernel with a radius of $R = 2\sigma$, indicating that the proposed smooth kernel offers a more favorable combination of isotropy and locality. Practically speaking, we would recommend values of $\sigma = 3$ and $c = 0.01$ since these are already in the region of diminishing returns. Finally, the modular nature of the MC algorithm means that it should be possible to incorporate the proposed kernel into existing codes with minimal effort.

Acknowledgements

This work was performed under the auspices of the US Department of Energy by Lawrence Livermore National Laboratory under Contract DE-AC52-07NA27344, and the authors were supported by US DOE Office of Basic Energy Sciences, Division of Materials Science and Engineering. Additional support for J.K.M. in the form of a Lawrence Postdoctoral Fellowship is also acknowledged.

References

[1] M. Anderson, D. Srolovitz, G. Grest, P. Sahni, Acta Metallur. 32 (1984) 783.
[2] D. Srolovitz, M. Anderson, P. Sahni, G. Grest, Acta Metallur. 32 (1984) 793.
[3] D. Srolovitz, M. Anderson, G. Grest, P. Sahni, Acta Metallur. 32 (1984) 1429.
[4] G. Grest, D. Srolovitz, M. Anderson, Acta Metallur. 33 (1985) 509.
[5] D. Srolovitz, G. Grest, M. Anderson, Acta Metallur. 33 (1985) 2233.
[6] A. Rollett, D.J. Srolovitz, M. Anderson, Acta Metallur. 37 (1989) 1227.
[7] A. Rollett, W. Mullins, Scr. Mater. 36 (1997) 975.
[8] Q. Yu, S.K. Esche, Mater. lett. 57 (2003) 4622.
[9] O. Ivasishin, S. Shevchenko, N. Vasiliev, S. Semiatin, Acta Mater. 51 (2003) 1019.
[10] D. Zöllner, P. Streitenberger, Scr. Mater. 54 (2006) 1697.
[11] G.L. Thomas, R. De Almeida, F. Graner, Phys. Rev. E 74 (2006) 021407.
[12] A.B. Bortz, M.H. Kalos, J.L. Lebowitz, J. Comput. Phys. 17 (1975) 10.
[13] G. Hassold, E.A. Holm, Comput. Phys. 7 (1993) 97.
[14] G. Korniss, M. Novotny, P.A. Rikvold, J. Comput. Phys. 153 (1999) 488.
[15] S. Plimpton, M.C. Corbett Battaile, L. Holm, A. Thompson, V. Tikare, G. Wagner, X. Zhou, C.G. Cardona, A. Slepoy, 2009.
[16] A.D. Rollett, P. Manohar, Continuum Scale Simulat. Eng. Mater.: Fundam.-Microstruct.-Process Appl. (2004) 77.
[17] N. Metropolis, A. Rosenbluth, M. Rosenbluth, A. Teller, J. Chem. Phys. 21 (1953) 1087.
[18] D. Raabe, Acta Mater. 48 (2000) 1617.
[19] M. Nosonovsky, X. Zhang, S.K. Esche, Model. Simul. Mater. Sci. Eng. 17 (2009) 025004.
[20] L. Zhang, A.D. Rollett, T. Bartel, D. Wu, M.T. Lusk, Acta Mater. 60 (2012) 1201.
[21] E.A. Holm, J.A. Glazier, D.J. Srolovitz, G.S. Grest, Phys. Rev. A 43 (1991) 2662.
[22] A. Miyake, Contrib. Mineral. Petrol. 130 (1998) 121.
[23] Y. Kim, S. Hwang, M. Kim, S. Kwun, S. Chae, Mater. Sci. Eng.: A 408 (2005) 110.
[24] D. Zöllner, Comput. Mater. Sci. 86 (2014) 99.
[25] J. Von Neumann, Metal Interfaces, American Society for Metals, Metals Park, OH, 1952, p. 108.
[26] W. Mullins, J. Appl. Phys. 27 (1956) 900.
[27] F.Y. Wu, Rev. Mod. Phys. 54 (1982) 235.
[28] L. Onsager, Phys. Rev. 65 (1944) 117.
[29] R.J. Glauber, J. Math. Phys. 4 (1963) 294.
[30] V.V. Bulatov, B.W. Reed, M. Kumar, Acta Mater. 65 (2014) 161.
[31] S. Raghavan, S.S. Sahay, Mater. Sci. Eng.: A 445 (2007) 203.
[32] O. Ivasishin, S. Shevchenko, S. Semiatin, Acta Mater. 57 (2009) 2834.